UT-S&E-LASER/DEC

Task Title: LASER HEATING OF COMPLEX GRAPHITE SURFACES BY HIGH REPETITION RATE NANOSECOND PULSES

INTRODUCTION

The excessive trapping of tritium in tokamak plasma-facing components is seen as a severe problem for the efficient operation of thermonuclear fusion reactors. A completely optical method of surface detritiation by laser ablation or laser heating can be offered for decontamination and internal surface cleaning of prospective International Thermonuclear Experimental Reactor (ITER). The commercially available powerful high repetition rate pulsed Nd-YAG lasers with laser radiation transported to the contaminated surface by the optical fiber are seen as good candidates for detritiation of all plasma-facing surfaces in tokamaks. The possibility to transport the laser beam to processed zone by the optical fiber allows to remove the laser system away from the contaminated zone and to carry out remote detritiation. The absence of the direct contact with the contaminated surfaces that ensures the personnel safety, the reduced waste volume, the accessibility of the laser beam to the shadowed areas, and a possible complete automation of the process are the most attractive features of laser decontamination.

To characterize the properties of the co-deposited carbon layer and of the native surface of manufactured graphite tiles, the thorough laser heating measurements with the pyrometer were performed. A specially developed infra-red pyrometer system was used for the surface heating measurements to study high repetition rate laser heating. A theoretical model of laser heating of complex surfaces with the boundary layer by periodically repeating nanosecond laser pulses was developed. The model allows to make 3D simulations of laser heating on large scales both in time and space. To obtain the detailed comparison of the experimental and calculation results, the theoretical model was extended to the case of intermediate heat contact between the layer and the substrate.

2005 ACTIVITIES

The experiments on laser heating of graphite tiles with a co-deposited carbon layer were made for Tore Supra tile and Textor tile. In the latter case, the experiments were made in different places on the tile with apparent different co-deposited layer properties (friability, contact with the substrate). Some results of the pyrometer measurements are shown in figure 1(a – f). The temperature traces in panels (a) and (b) are quite similar. It testifies to the fact that the Tore Supra co-deposit is rather thin (similar to the case (b) of Textor tile) or even thinner (because the minimal temperature in figure 1a seems lower than the one on figure 1b). Both temperature traces show a slow increase in the minimal temperature, which, however, does not exceed the minimal threshold of the pyrometer (at least, during laser heating). This impedes an effective comparison of the results of these measurements with the calculations. The case of figure 1c is more informative, because minimal heating temperatures are above the minimal threshold temperature of the pyrometer and very stable from ~10th laser pulse. Such minimal temperature behavior indicates that ablation is already in progress. For this reason, the experimental results in panels (d), (e) and (f) seem the most suitable for the modelling. From figure 1d, these results look very reproducible where two different measurements with different heating time in the same place on the tile are superimposed. For the case of figure 1d, similar to the one of figure 1c, the ablation seems to be in progress beginning from ~30th laser pulse. This conclusion can be made on the basis of saturation of the minimal heating temperature in this time range. The cutting the experimental results for the heating temperature from the top corresponds to the maximal threshold of the pyrometer. Thus, further on, the main attention is paid to the modelling of the experimental results in panels (e) and (f). These results were obtained with laser heating of neighboring but different places on plasma-facing surface of Textor graphite tile with a thick co-deposited layer (10-50 µm) being weakly adhered to the substrate.

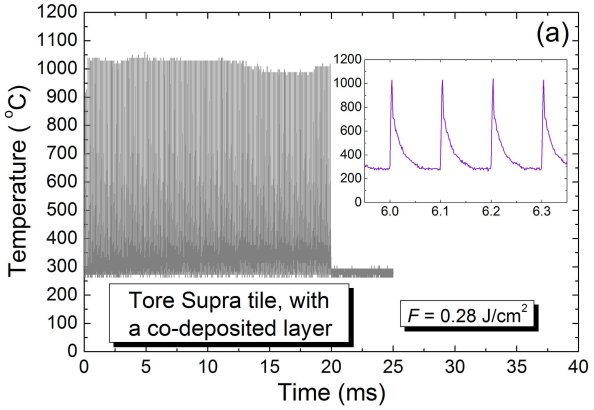

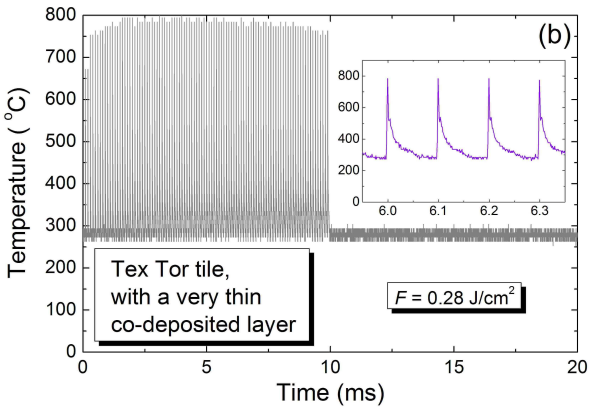

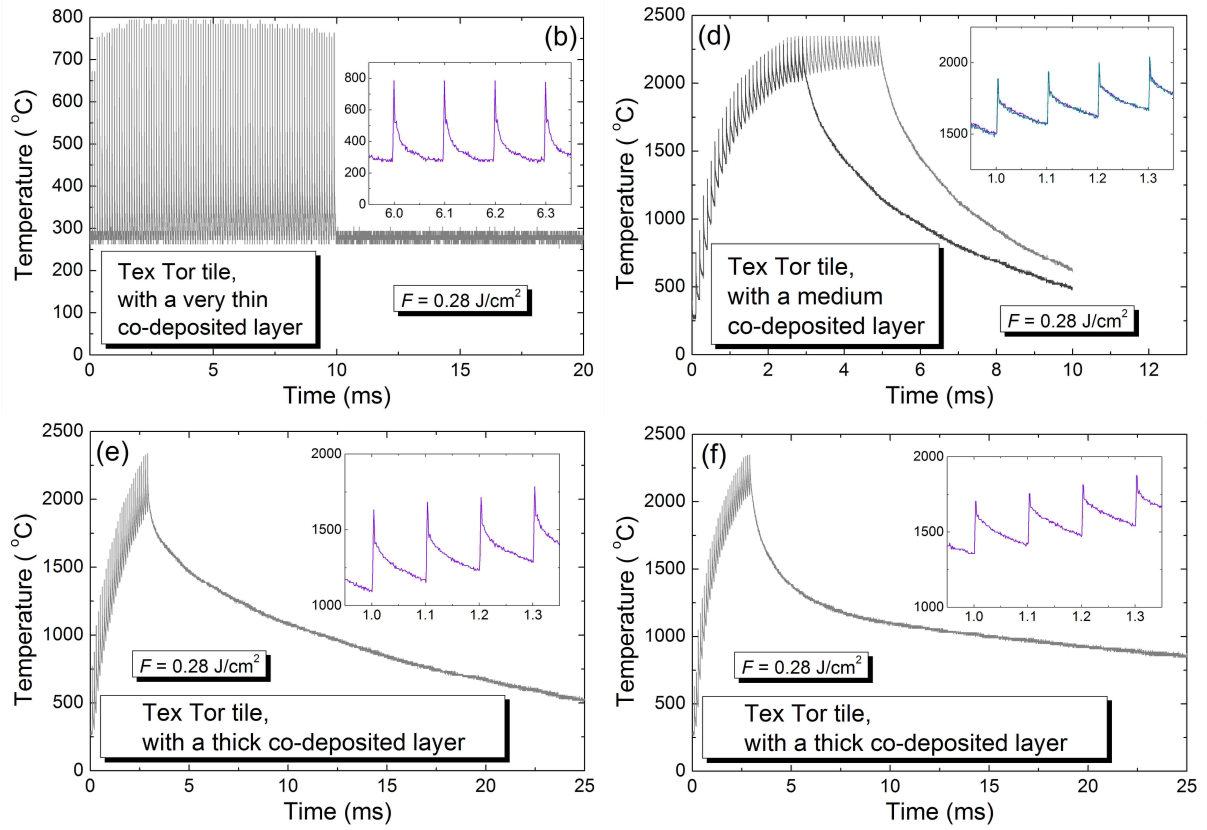

Figure 1: Panels (a) – (f) present the results of the pyrometer measurements on laser heating of plasma-facing surface of graphite tiles from Tore Supra (a) and from Textor (b) – (f). In the latter case, the different panels correspond to different places on the tile. The qualitatively indicated thickness of the co-deposited carbon layer was estimated only visually.

Figures 2 and 3 present the modelling of experimental temperatures obtained with a pyrometer (figure 1e and 1f, respectively). Figure 2a shows the best fit for the experimental temperature trace presented in figure 1e. The four parameters of the fit are as follows: the layer porosity p_L = 0.25, the layer thermoconductivity k_L = 0.12 W/(m·K), the layer thickness d = 16 μm, and the heat transfer coefficient of the layer/substrate interface h = 2.5 $\times 10^3$ W/(m^2·K). This set of the adjusting parameters seems unique (within both the fit and model accuracy).

The curvature of the minimal temperatures profile is defined mainly by porosity p_L of the layer. The slope of the relaxation curve tail (after the laser is switched off) is defined mainly by the heat transfer coefficient h. The heating temperature scale is defined by the layer thermoconductivity k_L. The global profile of the temperature trace (the coupling of the heating and relaxation parts of the global profile) depends on the layer thickness d.
The ablation seems to take place by the end of the heating. This conclusion can be made because the maximal calculated heating temperature reaches the sublimation temperature of graphite and it prevents to fit perfectly the final heating stage. Thus, the reliability of the adjusting parameters may be partially lost and, in particular, might be the reason that the calculated cooling curve does not perfectly correspond to the experimental one (figure 2b).

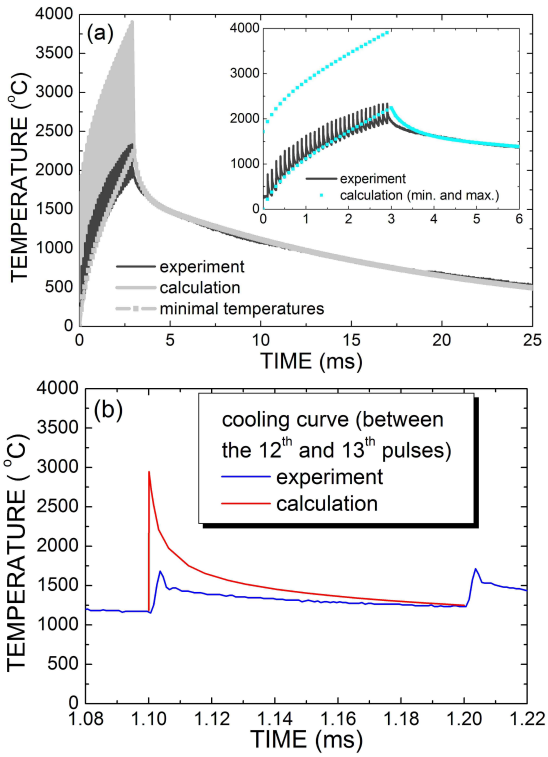

Figure 2: The modelling of the experimental temperature trace presented in Fig. 1e (plasma-facing surface of Textor tile with a co-deposited layer). The layer parameters resulting in the best fit are as follows: p_L = 0.25, k_L = 0.12 W/(m·K), h = 2.5×10^3 W/(m^2·K), d = 16 μm. Panel (a) presents the global temperature profile, and panel (b) shows the cooling curve between two adjacent laser pulses.

The similar situation takes place in the case of figure 3, where modelling of the experimental temperature profile presented in figure 1f is shown. The experimental results of figure 1e and 1f were obtained in different but neighboring places on plasma-facing surface of Textor tile. Thus, the layer thickness d was close to 15 µm for both cases. On the other hand, the porosities (or, equivalently, the densities) of the carbon layer in two places seem different. The best fit for the case of figure 3 corresponds to $p_L = 0$. In other words, in the second case the layer is more compact than the manufactured porous graphite. In the second case, the heat transfer coefficient is significantly lower and is $h = 0.9 \times 10^3$ W/(m^2·K). It means that in this case, the layer is poorly adhered to the substrate. And again, the ablation apparently takes place by the end of the heating, which may be even more effective if compared with the case of figure 2. This correlates with the lower heat transfer coefficient h. For both cases, thermoconductivity of the carbon layer is very low if compared with the thermoconductivity of graphite substrate. The explanation of this specific behavior can be the subject of a special study.

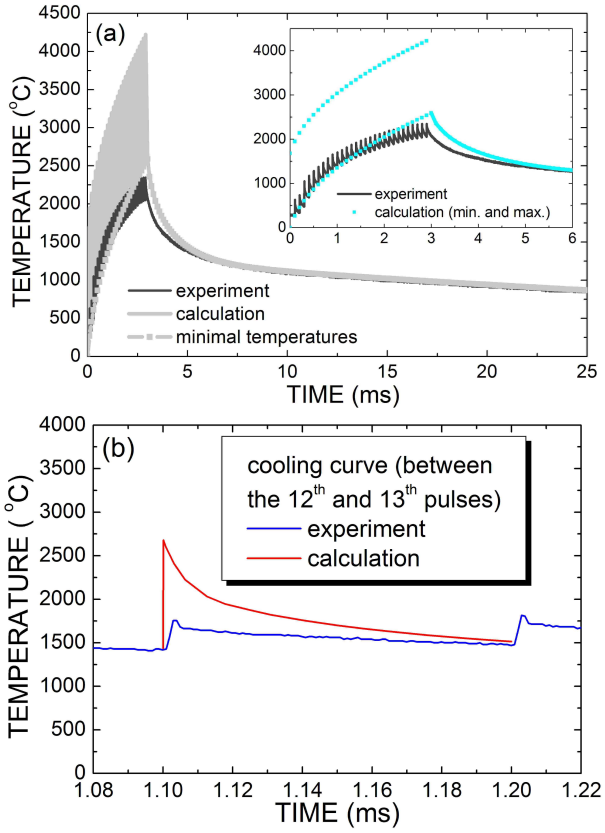

Figure 3: The modelling of the experimental temperature trace presented infigure 9f. The layer parameters resulting in the best fit are as follows: $p_L = 0$, $k_L = 0.05$ W/(m·K), $h = 0.9 \times 10^3$ W/(m^2·K), d = 15 µm. Panel (a) presents the global temperature profile, and panel (b) shows the cooling curve between two adjacent laser pulses.

CONCLUSIONS

The theoretical model of laser heating of complex surfaces (graphite or metal substrate with a co-deposited boundary layer intermediately adhered to the substrate) by repeating laser pulses is developed. The previously developed laser heating model with only two limiting cases of adhesion (completely perfect and completely imperfect heat contact between the layer and the substrate) was extended to the case of intermediate adhesion. It was also used to interpret and simulate the experimental results obtained in CEA Saclay (LILM) on laser heating of the graphite surfaces without and with a co-deposit layer from different tokamaks, and also to adjust some optical and thermo-physical parameters of manufactured graphite. The main results are as follows:

- 1. The characterization of the graphite parameters was made. On the basis of the experimental ablation thresholds, the laser absorption coefficient of manufactured graphite was estimated surprisingly low as 3.75×10^6 m^{-1}.

- 2. The simulations of laser heating of both the backside surface and the plasma-facing surface of graphite tiles from different tokamak installations were performed. The experimental results on laser heating of the backside surface of graphite tiles were simulated with a good agreement not only for the surface preprocessed by laser ablation, but also for the original (non-preprocessed) surface with unexpected boundary layer with the properties being different from those of the bulk. The specific unexpected features of laser heating of backside surface of Tore Supra graphite tiles were modeled and interpreted. The fit of laser heating experiments on TexTor tiles with a co-deposited layer is made with a rather good agreement.

- 3. It was ascertained that modelling of the experimental temperature profiles obtained with pyrometer measurements can allow to adjust all the unknown parameters of the co-deposited layer. It was established that four adjusting parameters (h, d, p_L, k_L) can be determined, in principle, from the fit of the simulated results to the experimental ones, providing full characterization of the boundary (co-deposited) layer.

- 4. The laser heating model was also validated by simulations of the laser heating of paint and cement.

On the basis of the simulation results, new experiments can be proposed to obtain detailed characterization of both graphite and a co-deposited layer.

REPORTS AND PUBLICATIONS

[1] A. Semerok, S.V. Fomichev, F. Brygo, J.M. Weulersse, P.-Y. Thro, “Laser heating of complex graphite surface by high repetition rate nanosecond pulses”, CEA Report, DPC/SCP/LILM/2006/170-A, 36 pages.

[2] A. Semerok, S.V. Fomichev, F. Brygo, J.-M. Weulersse, P.-Y. Thro, Ch. Grisolia, “Surface heating by pulsed repetition rate nanosecond lasers”, invited presentation on the LTL Conference, Plovdiv, Bulgaria, 2005, will be published in SPIE Proceedings 2006, 8 pages.

[3] A. Semerok, F. Brygo, S.V. Fomichev, F. Champonnois, J.-M. Weulersse, P.-Y. Thro, P. Fichet, Ch. Grisolia, “Laser detritiation and co-deposited layer characterisation for future ITER installation”, ENC Proceedings, Versailles, France, 2005.

TASK LEADER

Alexandre SEMEROK

DEN/DPC/SCP/LILM
CEA-Saclay
F-91191 Gif-sur-Yvette CEDEX

Tel. : 33 1 69 08 65 57
Fax : 33 1 69 08 78 84

e-mail : alexandre.semerok@cea.fr

UT-S&E-LiPbwater

Task Title: ANALYSIS OF THE CONSEQUENCES OF A COMMON FAILURE OF THE TEST BLANKET MODULE AND WATER BLANKET IN ITER

INTRODUCTION

Roughly, 500 water blankets are surrounding the vacuum vessel of the ITER reactor in order to remove the heat by a water circulation. The water temperature enters at a temperature of 100°C and is heated up to 150°C under a pressure of 30 bar. The water is in the liquid phase.
Furthermore, a Test Blanket Module (TBM) is surrounding the vacuum vessel in order to allow the tritium production by a neutronic reaction with the metal liquid Pb/Li present in the TBM. This liquid occupies a volume of 0.324 m^3, at a temperature of 550°C and a relatively low pressure comprised between 2 to 5 bar. The TBM is cooled down by a helium circulation, whose inlet temperature is 300°C and the outlet temperature 500°C under a pressure of 80 bar. The TBM total volume is 0.7 m^3.
In the framework of the safety analysis of ITER, the consequences of a common failure of the TBM and a few water blankets have to be investigated. It would result a hypothetical thermal interaction between the liquid metal Pb/Li and the liquid water in the vacuum vessel. The contact between these two liquids at relatively high temperature could yield a thermal interaction between them. The water will vaporize and thus pressurize the vacuum vessel, designed to withstand a maximum pressure of 2 bar. If such pressure were reached, the integrity of the vessel would be challenged. The purpose of the study is to investigate the phenomenology of this scenario.

2005 ACTIVITIES

The objective of the 2005 work was to analyze the consequences of such an interaction and to specify a method to calculate it.

CHEMICAL REACTION

It is useful to recall what will result from the contact between water and Pb/Li.
The contact between water and Pb/Li at which temperature in a low-pressure vessel will make the water vaporize.
Two types of accidents will also occur in the blanket module of a fusion reactor : a small leakage or a large leakage. In both cases, the chemical reaction that takes place is [1]:

Reaction in the presence of excess water:
$2Li + 2H_2O \rightarrow 2LiOH + H_2 \qquad \Delta H = -29\,MJ/kg - Li\ at\ 25°C$
Reaction in the presence of excess lithium:
$2Li + H_2O \rightarrow Li_2O + H_2 \qquad \Delta H = -22\,MJ/kg - Li\ at\ 25°C$

These chemical reactions are exothermic, inducing an increase of the pressure in the module blanket and threatening its integrity.

FIRST STUDY

The first study consists in analyzing the consequences of a simultaneous failure in the TBM and a few blankets with an excess of Pb/Li or water. This could yield a strong interaction between Pb/Li and water in the vacuum vessel. The thermal effect will be studied, not the consequences of hydrogen formation, which takes place later.

Excess of Pb/Li

Assuming that a pre-existing pool of Pb/Li is already present in the vacuum vessel (the initial pressure being close to 0), the contact results in water vaporization, followed by the production of solid lithium oxide and hydrogen. The situation is plotted figure 1.

The question is to determine the amount of water necessary to produce a resultant pressure of 2 bar due to the water vaporization. This preliminary work is based on a thermodynamic approach, namely a thermal equilibrium between water and Pb/Li.

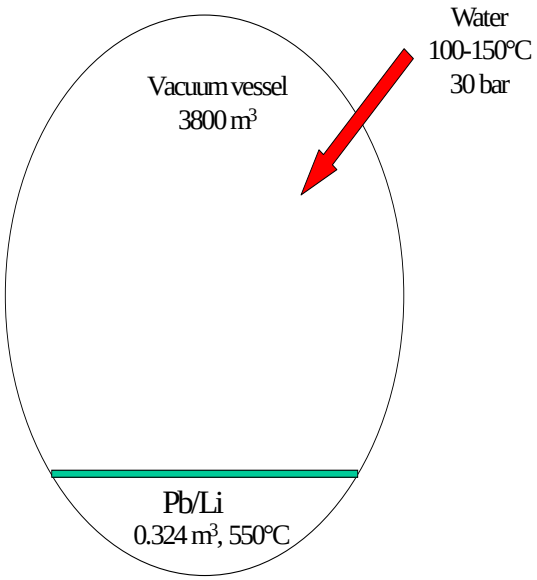

Figure 1: Vacuum vessel (excess Lithium)

Excess of water

If a pre-existing pool of water is present in the vacuum vessel with a lithium leak in the pool, aqueous lithium hydroxide and hydrogen gas will be produced. This second case is represented figure 2.

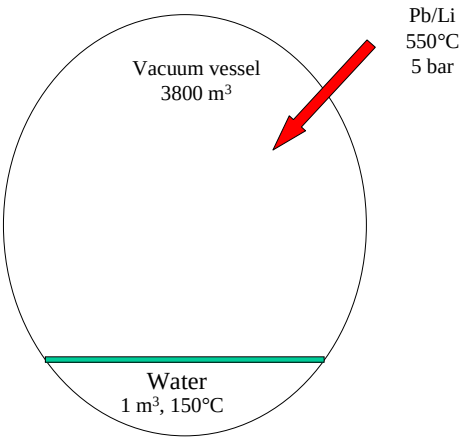

Figure 2: Vacuum vessel (excess water)

SECOND STUDY

The second study is similar to the previous one, except that helium is taken into account. The impact on the water amount to reach the maximum allowable pressure is investigated in these conditions.
The conditions are recalled figure 3.

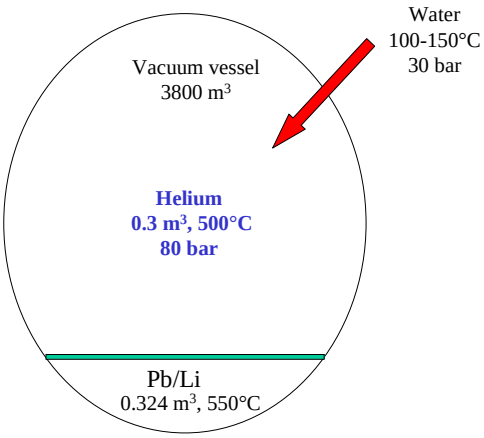

Figure 3: Vacuum vessel with helium

2006 FORESEEN STUDY

These two studies were estimated on a thermodynamic viewpoint in 2005 in order to give a first evaluation on the consequences of the Pb/Li and water interaction. Only stationary conditions were studied.

In 2006, it is proposed to follow this analysis by a refined modeling of the system with the SIMMER code [2]. The kinetics aspects of the mixing between the two liquids will be taken into account. The initial phase after the contact of the two liquids, which is subjected to the apparition of pressure peaks, will be investigated and the results will be compared to the present ones.

These kinds of Interaction between Pb/Li and water have already been calculated with the SIMMER code in the past. In particular, the interpretation of the LIFUS program was performed with this code [3]. The 2006 work will be an adaptation of these previous studies.

2005 THERMODYNAMIC STUDY

The main results of the 2005 work are presented hereafter.

VESSEL PRESSURIZATION WITHOUT HELIUM

The Pb/Li liquid metal is supposed to be initially under a pressure of 1 bar and a temperature of 550°C, the water being at 30 bar and 150°C.

Previous study

In the framework of the initial ITER project, the study was already performed with the two codes LINT and MELCOR [1] for similar conditions. At that time, water and not helium was chosen to cool down the TBM, so that the risk of a Pb/Li and water interaction was much higher. Furthermore, the vessel size was smaller; temperature and pressure were also different. In case of water excess in the vacuum vessel, a lithium leak with a 38 kg/s flowrate leads to a linear pressurization of the vessel up to the water boiling, obtained 125 seconds after onset. The design pressure of the vessel was reached in 50 s and the initial Pb/Li pressure of 5 bar was obtained after 125 s.

In case of a Pb/Li excess, the vessel failure is also reached within a matter of minutes. According to the initial Pb/Li mass, the failure time can decrease from 900 s to 100 s.
Considering these large flowrates, the vessel pressurization was extremely rapid. The present configuration is different since such large flowrates cannot be encountered.

The water vaporization

Considering the mixture of the two liquids, the possibility of complete water vaporization is checked with the present configuration.

If a complete mixing of the two fluids at a constant pressure were assumed, taking into account the water vaporization, the final temperature would be given by the equality of the heat exchanges.

The thermo-dynamical characteristics of water and Pb/Li and initial conditions are summarized Table 1.

Table 1: Properties of the two liquids/ initial conditions

	Water	Pb/Li
Volume	1000 m^3	0.324 m^3
Density (standard P, T)	1000 kg/m^3	9321 kg/m^3
Initial temperature	150°C	550°C
Initial pressure	30 bar	2-5 bar
Cp liquid	4180 J/K/kg	190 J/K/kg
$V_{aporization}$ (5 bar)	151.11°C	978°C
Initial temperature	150°C	550°C
Initial pressure	30 bar	2-5 bar

Two cases mentioned above; are investigated.

Water initially present in the vacuum vessel

Initially, 1 m^3 of water at a temperature of 150°C is present in the vacuum vessel. The Pb/Li liquid is injected at a temperature of 550°C.
As the water volume is very limited, the only way to increase the pressure in the vessel is to completely vaporize the water, then increase the water vapor. Using the perfect gas law, the temperature necessary to pressurize the vessel is of the order of $T = \frac{P \cdot V}{n \cdot R} \approx 2 \cdot 10^6 K$, which is unrealistic, since the Pb/Li temperature is 550°C.
There is therefore no risk of vessel pressurization if the water volume is limited. Since the vapor vaporization is unlikely, the probability of some pressure peaks is also low. Therefore, this case will not be investigated by detailed calculations.

Pb/Li initially present in the vacuum vessel

In case of a water injection in the vacuum vessel, initially filled with a mass of 0.324 m^3 of Pb/Li and a temperature of 550°C, the situation is different from the previous one. When water is injected in the vessel; the heat from Pb/Li will be transferred to the water.
Initially the vessel is not pressurized, so that water will be totally vaporized until the saturation temperature that corresponds to a pressure of 2 bar, namely 120°C. Then, this vapor will be heated until 150°C. If the water vapor is assumed to remain at the saturation pressure, a pressure of 5 bar will be reached.
The thermo-dynamical properties of water under 2 and 5 bar are given table 2.

Table 2: Water properties under 2 and 5 bar

Water	2 bar		5 bar	
Temperature (°C)	120 °C	150°C	120 °C	150°C
Density (kg/m^3)	1.1	1.02	944	918
Enthalpy (kJ/Kg)	2706	2770	505	633

The perfect gas law gives the amount of water necessary to reach the water saturation pressure at 150°C:
$P \cdot V = n \cdot R \cdot T$
Hence:
$P_{sat} = 0.93 \cdot n$ with n the number of H_20 moles.
For this temperature of 150°C under the saturation pressure of 5 bar, the water mass that can be vaporized is therefore around 9700 kg.
This calculated mass of 9700 kg corresponds to a volume of 10 m^3 of water under a pressure of 30 bar and a temperature of 150°C.
This value is coherent with the LINT and MELCOR calculations in the case of a water injection in the Pb/Li liquid [1, page 12]. The mass necessary to cause an initial pressurization was evaluated in this report to 8000 kg.
In the present calculation, the vessel failure is not considered. Since the water will be pressurized as long as it is coming into the vessel, it means that the vessel could fail even without any lithium interaction [1, page 10].
The design pressure of 2 bar would be reached with the 2/5 of the 9700 kg water mass, namely 3880 kg.

Although this water amount is quite large, further investigation would be needed to study the transient effects that will develop during the process of water vaporization. Indeed, pressure peaks are expected to occur during the mixing phase that could damage the vessel structure.

CONCLUSIONS

This specification report was aimed at presenting the question raised by a possible interaction between Pb/Li and water and recalling previous evaluations made in another context. Then, the water mass necessary to endanger to vacuum vessel integrity was estimated. Although this approach yields rapid results, it only corresponds to steady-state conditions that take into account -neither the transient mixture process -nor the system geometry where the mixture occurs. Consequently, it is proposed to pursue this study in 2006 by a complete modeling of the control volume of the vacuum vessel. The thermal interaction could be more precisely estimated and the pressures exercised on the vessel better calculated.

REFERENCES

[1] Computer Modeling for Lithium Safety in Fusion Systems: LINT and MELCOR, T.T Utschig and M.L Corradini (june 1999) - Fusion Technology Institute University of Wisconsin

[2] SIMMER-III : a computer code for LMFR core disruptive accident analysis Version 2.H model summary and program description S. Kondo et al (november 2000) JNC TN9400 2001-002

REPORTS AND PUBLICATIONS

[3] "Recalculation of the LIFUS experiment with the 3D version of SIMMER" (interaction between lithium-lead and water) T. Cadiou (february 2005) CEA/DEN/CAD/DER/SESI/LCSI/NT DO1 14/01/05

TASK LEADER

Thierry CADIOU

DEN/DER/SESI/LCSI
CEA-Cadarache
F-13108 Saint-Paul-lez-Durance Cedex

Tel. : 33 1 42 25 66 17
Fax : 33 1 42 25 71 87

e-mail : thierry.cadiou@cea.fr

UT-S&E-Tritium-Impact

Task Title: IMPACT OF CONTAMINATION WITH TRITIUM AT CELL LEVEL

INTRODUCTION

Ionizing radiation produces different kinds of damages on DNA among them oxidative stress and double strand breaks (DSB). DNA damages may lead to genetic alterations which could result in severe pathologies. DSB are the most toxic lesions, which can also be induced by DNA replication arrest. Accumulation of these lesions can trigger cell cycle checkpoints and programmed cell death but non-accurate repair of DSB can lead to genetic rearrangements. Homologous recombination (HR) and non-homologous end-joining (NHEJ) are the main processes for DSB repair.

To produce DNA damages, external irradiation requires sufficient energy to reach the nucleus. In such conditions, tritium radiation cannot reach the DNA. However, organically bound (OBT) tritium can be incorporated into the cell resulting in an in situ chronic irradiation, which is now able to reach the biological target. Because of the low disintegration energy of Tritium, its biological effects cannot come from external exposure but from integration into tissue resulting in auto-irradiation. Consequently, the energy deposition is concentrated in the sub-cellular compartment, and may amplify the biological consequences. In this situation, the low penetration of the beam becomes an amplification factor: indeed, when tritium is incorporated into the nuclear DNA (with tritiated nucleotides), due to the short course of the rays, 70 % of the energy is deposited into the nucleus. The impact of Tritium on DNA integrity directly derives from the deposited energy and not from any chemical poisoning since tritium only generates water. However association with another contaminant, which affects cell response, can produce synergistic effects. Moreover, it is also possible that tritium incorporation engages cells in a response that could be inappropriate for a concomitant associated stress.

Our project aimed to study the impact of contamination with tritium on cell survival, cell cycle, mutagenesis, HR and NHEJ. Moreover our project will study the impact of tritium contamination on the cell response to an additional independent and well controlled DSB.

In 2005, we evaluate the impact of sub-lethal doses of contamination by ^{3}H-thymidine on cell survival, cell cycle, DNA double-strand breaks (DSB), homologous recombination (HR) and mutagenesis, in hamster CHO cells.

2005 ACTIVITIES

Cells were cultured in the presence of different specific activities of labeled thymidine. After 20 hours, when incorporation reached a plateau and over 95% of cells contained labeled nucleotides, radioactivity incorporated into the DNA was counted in trichloroacetic acid (TCA) precipitates. In parallel cultures, cell cycle analysis, viability (cloning efficiency), γ-H2AX or Rad51 foci (immuno-fluorescence), mutagenesis and recombination frequency were measured (figure 1).

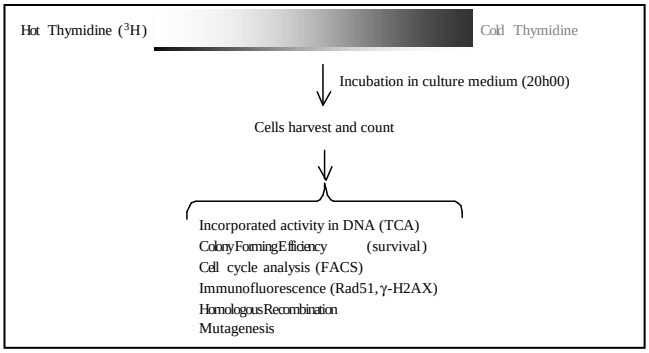

Figure 1

Contamination with ^{3}H-nucleotides and measure of cell cycle, survival, mutagenesis and HR. Impact of mutation in DSB repair pathways.

Measure of survival and HR

Incorporation of ^{3}H-thymidine did not significantly affect viability for doses lower than 10^{5} dpm/10^{6} cells. Higher incorporation resulted in a slight reduction of viability to 60 % (figure 2A).
In previous studies, we and other have shown that ionizing radiation and DSBs stimulate HR in p53^{-} cells (Lambert and Lopez, 2000; Liang et al., 1998; Saintigny et al., 1999; Wang et al., 1988) but at highly toxic doses (compare figures 3A and 3B). Indeed, γ-rays significantly induce HR but at doses leading 20 to 10% survival (figure 3B). In contrast, at poorly cytotoxic doses, strong HR induction was recorded for ^{3}H-thymidine incorporation (figure 3C). Importantly, the HR plateau induction was reached for *doses lower than 3.10^{5} dpm/10^{6} cells*, i.e. for exposure allowing 80 % to 100 % survival (compare figures 3C and 2A). For doses allowing comparable levels of viability (80 to 100 %), no γ-rays-induced HR was recorded. Moreover, the maximum HR stimulation with highly cytotoxic γ-rays (6 Gy) was extremely low compared with the HR level induced by non-lethal contamination; such levels of HR induction cannot be reached with γ-rays since the extrapolated calculated doses would be too toxic (45 to 80 Gy).

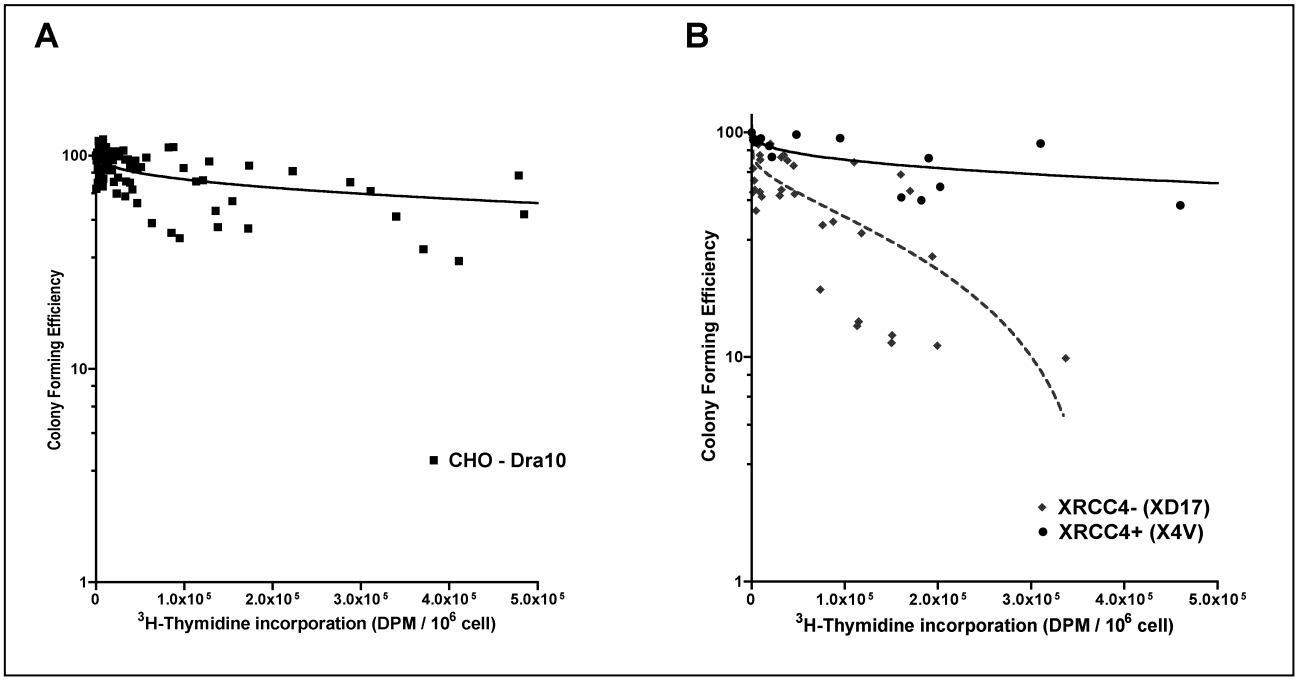

Figure 2

Measure of cell cycle

Cell cycle repartition was measured by classical methods. We showed that there is no effect on the cell cycle repartition of ^{3}H-thymidine incorporation until 1.10^{6} dpm/10^{6} cells. From that dose and upper, we measured a G2/M phase arrest. The G2/M checkpoint is generally under control of ATM or ATR signaling pathways. Caffeine incubation is able to inhibited G2/M arrest induced by either ATR or ATM. The G2/M block induced by of ^{3}H-thymidine incorporation was reversed by caffeine. Moreover, ATR signaling pathway inhibitor UCN-01 was able to inhibited G2/M arrest induced by ^{3}H-thymidine. Theses results were also confirmed by using a ATM defective mutant cell line. Taken together, theses data show that the incorporation of high doses of ^{3}H-thymidine (>1.10^{6} dpm/10^{6} cells) lead the cell to a G2/M arrest mediated by the ATR signaling pathway.

Mutagenesis

Mutagenesis was measured on two different loci: Na+/K+ pump ATPase, which monitors only point mutations, and HPRT which monitors both point mutations and long extent rearrangements. We measured a peak of point mutations for doses allowing 90 to 100 % of viability ($\leq$ to 10^{5} dpm/10^{6} cells). Surprisingly, no mutations by long extent rearrangements were scored in our assay. Taken together, these results suggest that oxidative stress may be responsible for mutagenesis induced by low incorporation of ^{3}H-thymidine.

Impact of DSB repair mutants

Since NHEJ mutants are highly sensitive to ionizing radiation, we measured the impact of labeled-thymidine incorporation on viability of an NHEJ-defective cell line (XD17) mutated in the xrcc4 gene (figure 2B). Whereas the CHO-DRA10 and the X4V (XD17, complemented with the XRCC4 cDNA) exhibited similar viability, xrcc4- cells show significantly higher sensitivity to ^{3}H-thymidine incorporation (figure 2B). At a dose of 2.10^{5} dpm/10^{6} cells, the viability of the xrcc4- cells was only 10 %, whereas it was 51 % and 82 % for XV4 and CHO-DRA10, respectively. The LD50 (Lethal Dose 50 %) dose was 7.10^{4} dpm/10^{6} cells for XD17 (xrcc4-) whereas it was 1.10^{6} dpm/10^{6} cells for XV4 or CHO-DRA10 (figure 2A and B). Thus xrcc4- cells are more than 14-fold more sensitive to the incorporation of ^{3}H-thymidine, than control cells. Taken together, these data show that cells defective in DSB repair by NHEJ are more sensitive to labelled nucleotide incorporation. However, these results are highly consistent with the fact that 70 % of the tritium energy was deposited into the nucleus

Effect of ^{3}H-nucleotides contamination on gamma-H2Ax and Rad51 assembly (nuclear foci)

γ-H2AX foci induction

After radiation, histone H2AX is phosphorylated and assemble into nuclear foci at the DSB sites ((Aten et al., 2004) and for review (Redon et al., 2002)). The γ-H2AX foci formation may be monitored by immunological staining then scored. Since the results above suggested that ^{3}H-thymidine induce DSBs, we thus analyzed the formation of γ-H2AX foci after incorporation of ^{3}H-thymidine, at non-lethal doses (figure 4A). The percentage of cells with γ-H2AX foci increased as a function of incorporated ^{3}H-thymidine but required more than 10^{5} dpm/10^{6} cells for detection (figure 4B). We then measured the mean number

of γ-H2AX foci per cell, after ^{3}H-thymidine contamination. Indeed, with γ-rays, a linear relationship exists between the number of γ-H2AX and the estimated number of DSBs (Rothkamm and Lobrich, 2003). This value will give us an extrapolated estimation of ^{3}H-thymidine-induced DSBs.

In CHO-DRA10 cells line the mean number of foci/cell evolved from 5 to 12 for incorporated doses comprised between 1.10^{4} to 5.10^{5} dpm/106 cells (figure 4C).

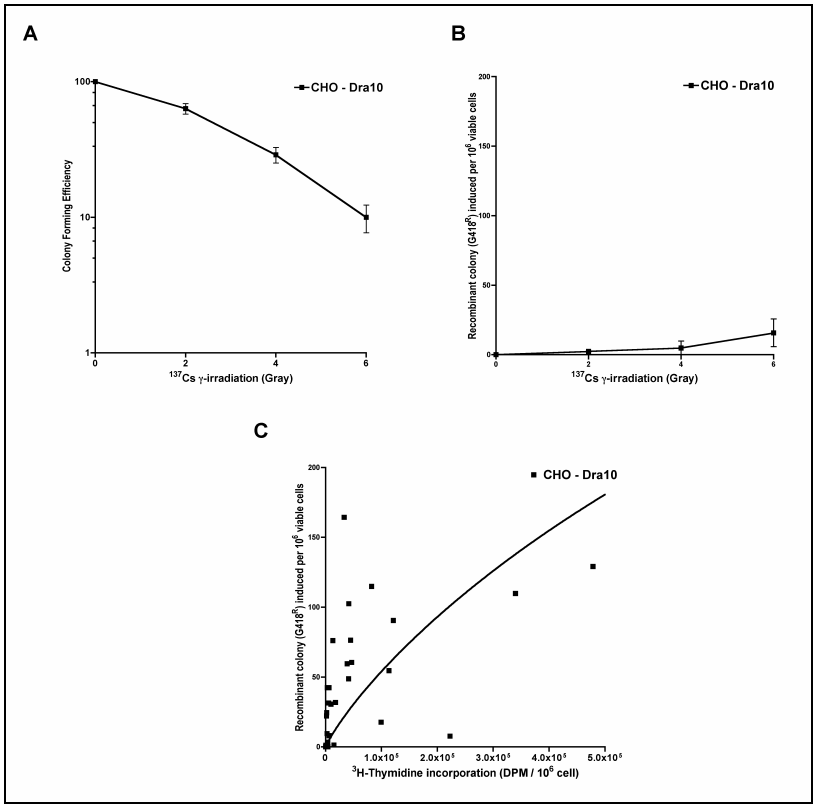

Figure 3

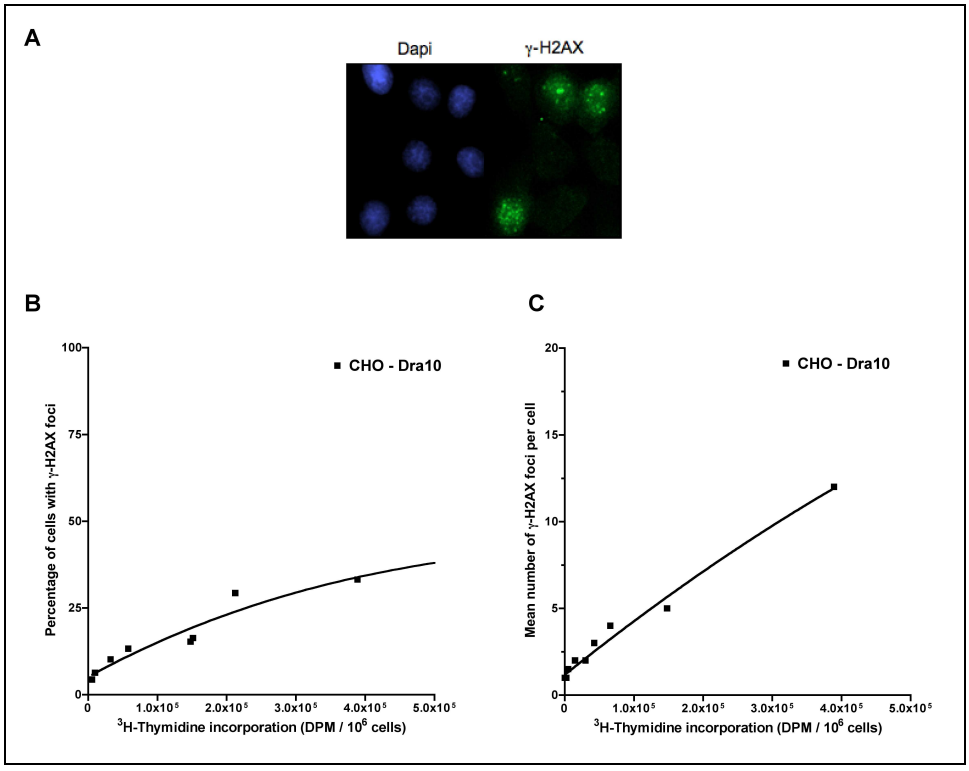

Figure 4

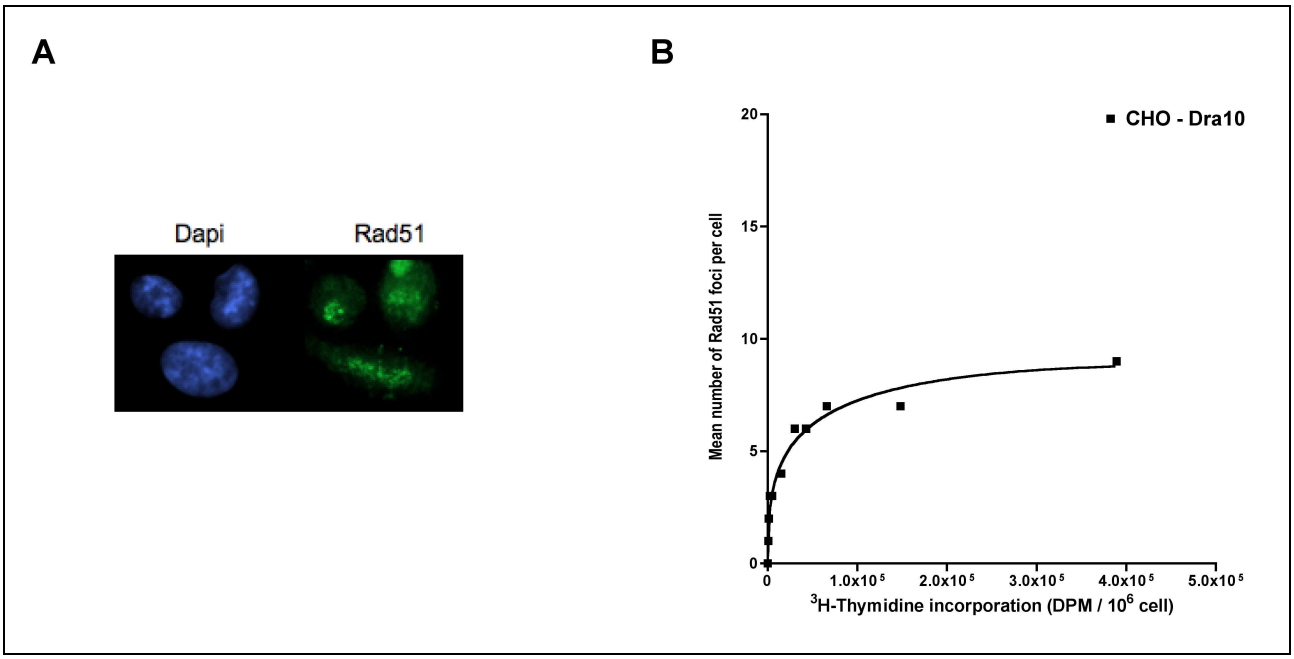

Figure 5

RAD51 foci induction

After genotoxic stress, the pivotal HR protein Rad51 assembles into nuclear foci at DNA damage sites, associated with γ -H2AX irradiated chromosome domains, which are thus thought to represent recombination/repair centers (Haaf et al., 1995). Rad51 foci assembly seems to represent a pre-requisite since until now, no HR events are recorded when Rad51 assembly is impaired.

We show here that ^{3}H-thymidine contamination induced Rad51 foci assembly (figure 4). Rad51 foci began to be detectable at a dose of 3.10^{4} dpm/10^{6} cells, then reached a plateau with 50 % of cells containing Rad51 foci at 1.10^{5} dpm/10^{6}. Importantly, the dose response of Rad51 foci assembly was highly consistent with those of HR induction (compare figure 4B and 2C).

CONCLUSIONS

We have analyzed the impact of ^{3}H-thymidine contamination at a molecular level. A precise subcellular compartment was targeted (the DNA molecule) and we identified some metabolic pathways responding to radioactive contamination, i.e. XRCC4 and RAD51 pathways. In addition, and very importantly, we show here that contamination by ^{3}H-thymidine induced a tremendous stimulation of HR, even in the absence of cell mortality. Such a HR stimulation level cannot be reached with γ-rays, which mainly kill the cells. At the incorporated dose used here, strong genetic effects (mutagenesis or HR) were recorded but no toxicity was observed in CHO cells. The fact that NHEJ mutant cells show increased sensitivity and that HR is stimulated in CHO-DRA10 cells supports the result that incorporated ^{3}H-thymidine produces DSB in the DNA as scored by γ -H2AX foci induction. On the basis of these considerations, the results presented here show that cell contamination with non-toxic doses of tritium may be hazardous for genetic stability. Thus, the remarkable survival of these contaminated cells associated to genetics alterations may increase the risk of: 1 - transmission of genetic modifications to the next generation and 2 - increase the risk of cancer (cancer cell should accumulated mutations and be viable to generate a tumour). Our work emphasizes the strong differences between an external ionizing radiation exposure and an internal radioactive contamination on biological consequences. The concept of dose of internal contamination in radiation protection may be re-evaluted.

REFERENCES

Aten, J. A., Stap, J., Krawczyk, P. M., van Oven, C. H., Hoebe, R. A., Essers, J., and Kanaar, R. (2004). Dynamics of DNA double-strand breaks revealed by clustering of damaged chromosome domains. Science *303*, 92-95.

Haaf, T., Golub, E. I., Reddy, G., Radding, C. M., and Ward, D. C. (1995). Nuclear foci of mammalian Rad51 recombination protein in somatic cells after DNA damage and its localization in synaptonemal complexes. Proc Natl Acad Sci U S A *92*, 2298-2302.

Lambert, S., and Lopez, B. S. (2000). Characterization of mammalian RAD51 double strand break repair using non lethal dominant negative forms. EMBO J *19*, 3090-3099.

Liang, F., Han, M., Romanienko, P. J., and Jasin, M. (1998). Homology-directed repair is a major double-strand break repair pathway in mammalian cells. Proc Natl Acad Sci U S A *95*, 5172-5177.

Redon, C., Pilch, D., Rogakou, E., Sedelnikova, O., Newrock, K., and Bonner, W. (2002). Histone H2A variants H2AX and H2AZ. Curr Opin Genet Dev *12*, 162-169.

Rothkamm, K., and Lobrich, M. (2003). Evidence for a lack of DNA double-strand break repair in human cells exposed to very low x-ray doses. Proc Natl Acad Sci U S A *100*, 5057-5762.

Saintigny, Y., Rouillard, D., Chaput, B., Soussi, T., and Lopez, B. S. (1999). Mutant p53 proteins stimulate spontaneous and radiation-induced intrachromosomal homologous recombination independently of the alteration of the transactivation activity and of the G1 checkpoint. Oncogene *18*, 3553-3563.

Wang, Y. Y., Maher, V. M., Liskay, R. M., and McCormick, J. J. (1988). Carcinogens can induce homologous recombination between duplicated chromosomal sequences in mouse L cells. Mol Cell Biol *8*, 196-202.

REPORTS AND PUBLICATIONS

Roche S., Saintigny Y., Meynard D. and Lopez B. S. Contamination with sub-lethal doses of labeled nucleotides (tritium or radiocarbone) induces double strand breaks and stimulates RAD51-dependant hyper-recombination in an inverse correlation with their energy. Paper to be submitted in 2006.

Saintigny Y. Interaction du tritium sur la réponse aux stress génotoxiques et la stabilité du génome. 3ème séminaire annuel du programme de recherche pluridisciplinaire (programme national inter-organismes) en Toxicologie Nucléaire Environnementale (ToxNuc-E), December 2005. Campus Michel Ange du CNRS, Paris – France. Oral communication

Saintigny Y., Roche S. and Lopez B. S. Impact d'une contamination au tritium sur la stabilité génétique. 6ème colloque des 3R, Réplication, Recombinaison et Réparation, June 2005. Giens – France.

TASK LEADER

Bernard S. LOPEZ

DSV/DRR/SRMC/LMR
CEA-Fontenay-aux-Roses
18, route du Panorama – BP 6
F-92265 Fontenay-aux-Roses Cedex

Tel. : 33 1 46 54 88 35
Fax : 33 1 46 54 89 55

e-mail : bernard.lopez@cea.fr